

RESEARCH

Open Access



Mechanical study of the safe distance between humerus shaft fracture and distal locking screws in antegrade nailing

Michele Coviello^{1*} , C. Gallo¹, V. Stragapede¹, F. Albano², F. Ippolito³, L. Macarini⁴, L. Stoppino⁴, V. Pesce¹ and G. Maccagnano¹

Abstract

Background Optimal positioning of distal locking screws in intramedullary humeral nailing remains uncertain, particularly the influence of the distance between the fracture plane and the proximal distal locking screw on construct stability. This study aims to evaluate the mechanical stability of humeral nailing under different fracture-to-screw distances and numbers of distal locking screws using finite element analysis and mechanical testing on bone models.

Methods A finite element model and mechanical testing on six sawbones models were performed under traction (500 N), compression (500 N), and torsion (3 Nm). Models were tested with two osteotomy distances from the proximal distal locking screw (2 cm and 5 cm) and with either one or two distal locking screws. Axial and torsional stiffness and fracture displacement were recorded and analyzed statistically.

Results Finite element analysis showed higher stress concentrations near the distal fracture fragment. Mechanical testing demonstrated that traction and torsional stability were significantly affected by fracture-to-screw distance ($p=0.006$ and $p=0.015$), while compression stability was influenced by the number of distal screws ($p=0.035$).

Conclusion A fracture-to-screw distance of 5 cm was associated with improved axial and torsional stability, while double distal screws enhanced compressive stiffness. These biomechanical results, although very promising, should be confirmed with clinical studies.

Keywords Humerus nailing, Mechanical study, Distal screw

*Correspondence:

Michele Coviello
michelecoviello91@gmail.com

¹Orthopaedics Unit, Department of Clinical and Experimental Medicine, Faculty of Medicine and Surgery, University of Foggia, Policlinico Riuniti di Foggia, 71122 Foggia, Italy

²Orthopaedic and Trauma Unit, Department of Basic Medical Sciences, Neuroscience and Sense Organs, School of Medicine, AOU Consorziale Policlinico, University of Bari "Aldo Moro", Piazza Giulio Cesare 11, 70124 Bari, Italy

³Orthopaedic and Traumatology Unit, "Di Venere" Hospital, Via Ospedale di Venere, 1, 70131 Bari, Italy

⁴Radiology Department, University of Foggia, Policlinico Riuniti di Foggia, 71122 Foggia, Italy



© The Author(s) 2025. **Open Access** This article is licensed under a Creative Commons Attribution-NonCommercial-NoDerivatives 4.0 International License, which permits any non-commercial use, sharing, distribution and reproduction in any medium or format, as long as you give appropriate credit to the original author(s) and the source, provide a link to the Creative Commons licence, and indicate if you modified the licensed material. You do not have permission under this licence to share adapted material derived from this article or parts of it. The images or other third party material in this article are included in the article's Creative Commons licence, unless indicated otherwise in a credit line to the material. If material is not included in the article's Creative Commons licence and your intended use is not permitted by statutory regulation or exceeds the permitted use, you will need to obtain permission directly from the copyright holder. To view a copy of this licence, visit <http://creativecommons.org/licenses/by-nc-nd/4.0/>.

Introduction

Humeral shaft fractures constitute 3–5% of all fractures, with an annual incidence ranging from 13 to 20 cases per 100,000 patients [1, 2]. Although conservative treatment has historically yielded favourable outcomes, with a consolidation rate of 97% [3], the growing demand for functional recovery and shortened rehabilitation periods has led to increased adoption of surgical interventions. However, this trend has been accompanied by an increase in postsurgical complications, including infections, rotator cuff injuries, radial nerve injuries (occurring in 11–25% of cases) [4] and pseudoarthrosis (affecting 8–12% of patients) [5].

Recent literature indicates that conservative treatment, employing braces or plaster, fails in approximately 33% of cases [6]. The surge in humeral shaft fractures, largely attributed to the ageing population, has spurred interest in surgical interventions such as open reduction and internal fixation (ORIF) and/or closed reduction and internal fixation (CRIF), as evidenced by comparative studies [7–9]. Intramedullary nailing has long been established as a viable surgical approach for lateral femoral neck fractures and, more recently, for humeral shaft fractures due to its minimally invasive nature with respect to the tissue and fracture biology. This approach is associated with a shorter consolidation time, reduced surgical duration, and diminished postoperative blood loss [7]. However, it is not without its drawbacks, as radial nerve injuries occur in approximately 20% of cases [10]. Additionally, pseudoarthrosis, a concerning complication, is

influenced by the biomechanical characteristics of the upper limb, which is subjected to torsional forces rather than axial loads.

According to Arbeitsgemeinschaft für Osteosynthesefragen (AO) principles, Perren's strain theory, and relative deformation theory [11], bone healing is influenced by various factors, including fracture type, orientation of the fracture plane, fracture gap, and osteosynthesis stability. In the context of intramedullary osteosynthesis, the diameter of the nail and the configuration of proximal and distal locking screws are crucial factors. While safety distances for distal locking in femoral intramedullary nails have been described in the literature [12], similar guidelines for humeral nailing are lacking. This is a significant issue, considering the risk of radial nerve injuries associated with distal locking screws [13].

The aim of this study is to biomechanically evaluate the influence of the fracture-to-screw distance and the number of distal locking screws on the primary stability of humeral intramedullary nailing. Understanding how these parameters affect axial, compressive, and torsional stiffness in a standardized sawbone model may support the refinement of implant configurations.

Methods

We conducted a biomechanical study via a preliminary finite element method (FEM) analysis [14]). This simulation technique allows complex physical phenomena to be studied quickly and inexpensively. The FEM analysis was carried out by the SOLIDWORKS Simulation program (3DS-Dassault System), which adopted geometric 3D graphic humeri models created based on X-rays (anterior to posterior (AP) and lateral views) and 3D graphic nail models based on the computer-aided design (CAD) model of a Dinamic T Humerus nail (Citieffe, Bologna, Italy) (Fig. 1), to extrapolate data concerning the fracture displacement and tensional bone and nail state (MPa). The geometric models were subjected to loading configurations of traction 500 N, compression 500 N and torsion 3 Nm (Fig. 2), as the principal forces acting on long bones [15]. The tension data were analysed based on the osteotomy level and by comparing the von Mises stress results by load group. The linear elastic isotropic properties [16, 17] of the reference materials were attributed to the geometric models, as reported in Table 1.

The study continued into the mechanical testing phase with three loading configurations—traction (500 N), compression (500 N) and torsion (3.00 Nm)—applied with a MTS 858 Mini Bionix universal test machine [18]. The sawbones and Dinamic T Humerus nail samples were subjected to loads that did not exceed the yielding limits, a choice made to avoid implant failure and to test the stability within the limits of elastic deformation. All implantation procedures were performed by



Fig. 1 Geometric sawbone–Dinamic T Humerus nail model made with the SOLIDWORKS Simulation program (3DS-Dassault System) based on X-rays (AP and lateral view)

- A. TRACTION (500N, 2-5cm and 1-2 screw)**
B. COMPRESSION (500N, 2-5cm and 1-2 screw)
C. TORSION (3Nm, 2-5cm and 1-2 screw)

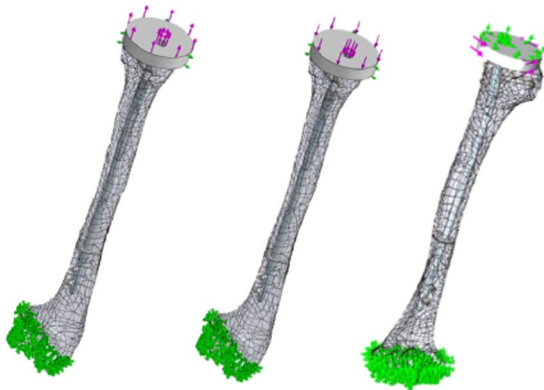


Fig. 2 FEM models and loading configuration

Table 1 Linear elastic isotropic properties attributed to the geometric models

	Poisson ratio	Elastic tensile modulus	Tensile strength
Digital bones	0,3	16,000 MPa	106 MPa
Digital Nail/Screw (Ti-6Al-AV)	0,34	113,800 MPa	860 MPa

the same orthopaedic surgeon who has more than 10 years of experience in traumatology: reaming epoxy composite/fiberglass sawbone models (sawbones 3404-4, Vashon Island, Washington) and implanting the Dinamic T Humerus nails (Ti-6Al-4 V, proximal $\phi 10$ mm, distal $\phi 7$ mm, 280 mm) with three cephalic proximal locking screws ($\phi 5$ – 45 mm) and two cortical locking screws ($\phi 3.5$ – 20 mm). For each test sample, a dedicated

resin mask for the models (ELANTAS MG 542) was made to allow proximal and distal gripping and guarantee the same stress conditions for the samples during the mechanical test. Six sawbones and Dinamic T Humerus nail baseline samples with double distal cortical locking screws were subjected to the four loading configurations (first RUN) to rule out failure events. Afterwards, an osteotomy of 1 mm was made to simulate a 12.A3 humeral shaft fracture (transverse fracture) according to the AO classification [19]. The samples were equally and randomly divided between the osteotomy levels (2 cm and 5 cm). Finally, we obtained six samples with a single cortical locking screw by removing the distal screw. The samples in the double and single cortical locking screw groups were subjected to mechanical testing at different times. Figure 3 shows the sample group subjected to mechanical tests. Axial and torsional stiffness data were extrapolated, and variations in the proximal mask–distal mask distance were measured by linear regression at the last of five loading/unloading cycles for three repetitions (RUN) for each sample. In addition, for the traction/compression tests, we recorded the variation in the fracture gap using an extensometer (model No. MTS 632.79 F-01) placed between the osteotomy fragments. The data, collected in triplicate, were subjected to normality analysis by the Shapiro–Wilk test, the homoscedasticity test via the Bartlett test, and subsequently to two-factor variance analysis with replication by analysis of variance (ANOVA). In conclusion, statistical significance was established through the ANOVA test, and a subsequent Bonferroni test was conducted to provide a comprehensive comparison among the four proposed sample configurations. All the statistical analyses were meticulously executed using MATLAB statistical software

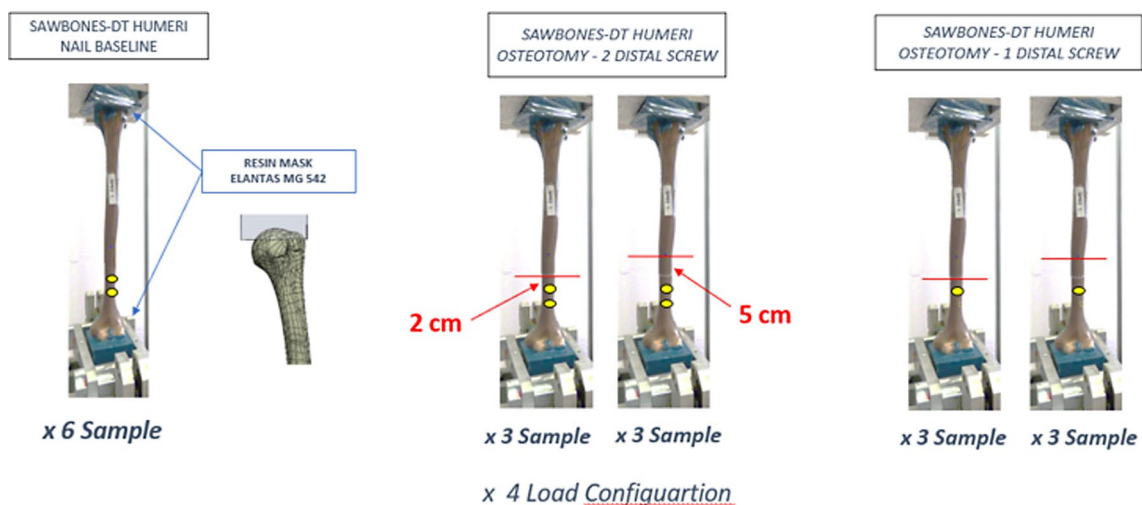


Fig. 3 Six sawbones–Dinamic T Humerus samples were divided in two groups according to osteotomy level; afterwards, the distal locking screw was removed to create two other research groups

(MathWorks Inc.). A predetermined threshold of significance was set at a p value less than 0.05.

Results

According to the FEM analysis, we reported a higher bone tension at the bone–device interface on the anterior surface of the distal fracture fragment for all loading configurations; greater bone tension was observed in the 2 cm osteotomy group for the traction 500 N group, while in the torsion 3 Nm group, there was a slight increase anteriorly near the first screw; posteriorly, the screws were equally stressed. When the distal locking screw was removed with a compression of 500 N, the tensile state of the bone changed, and the tension was anteriorly concentrated at the empty hole but posteriorly increased at the present screw (Fig. 4).

Along the entire cylindrical section, the tensile state of the nail appeared homogeneous (traction 500 N: 30 MPa in the 2 cm configuration; compression 500 N: 25 MPa in the 5 cm configuration); regarding torsion, it appeared higher at the osteotomy level (40 Nm), especially for the 2 cm osteotomy configuration, but remained below its yield point; as shown for a traction of 500 N (43 MPa), the increase in the tension at the osteotomy level was slightly less than that at the 5 cm osteotomy configuration (Fig. 5). The tension of the proximal distal locking screw was greater (traction 500 N: 55,37 MPa in the 2 cm configuration, 49,85 MPa in the 5 cm configuration; torsion was 65 Nm); regarding a compression of 500 N, the

tensions of the two distal locking screws were similar (50 MPa), but that of the first screw increased (65 MPa) after removing the second distal locking screw.

The displacement (mm) at the osteotomy level and load level is summarized in Table 2.

The displacement under a traction of 500 N was slightly lower in the 5 cm osteotomy configuration. There were no significant differences between the single and double distal locking cases, and no significant variations in the tension of the bone were noted. Displacement under a torsion of 3 Nm did not show any differences between the two osteotomy configurations. Instead, the displacement under a compression of 500 N was due to the type of distal lock; in fact, we reported a reduction of 10% (2 cm osteotomy) and 8% (5 cm osteotomy) from a single to double distal lock.

The experimental continued with mechanical tests, and according to the methods described above, we did not observe any cases of implant failure. Table 3 shows the average axial stiffness and displacement for a traction of 500 N. We performed two-factor variance analysis with replication (ANOVA), which revealed a statistically significant difference ($p=0.006$) in the association between the displacement of the fracture fragment and the osteotomy configuration. There was no significant difference in the displacement/number of distal screws ($p=0.280$) or the osteotomy/number of distal screws ($p=0.570$). The Bonferroni test revealed statistically significant differences for the 5 cm osteotomy/2 screw and 2 cm/1 screw

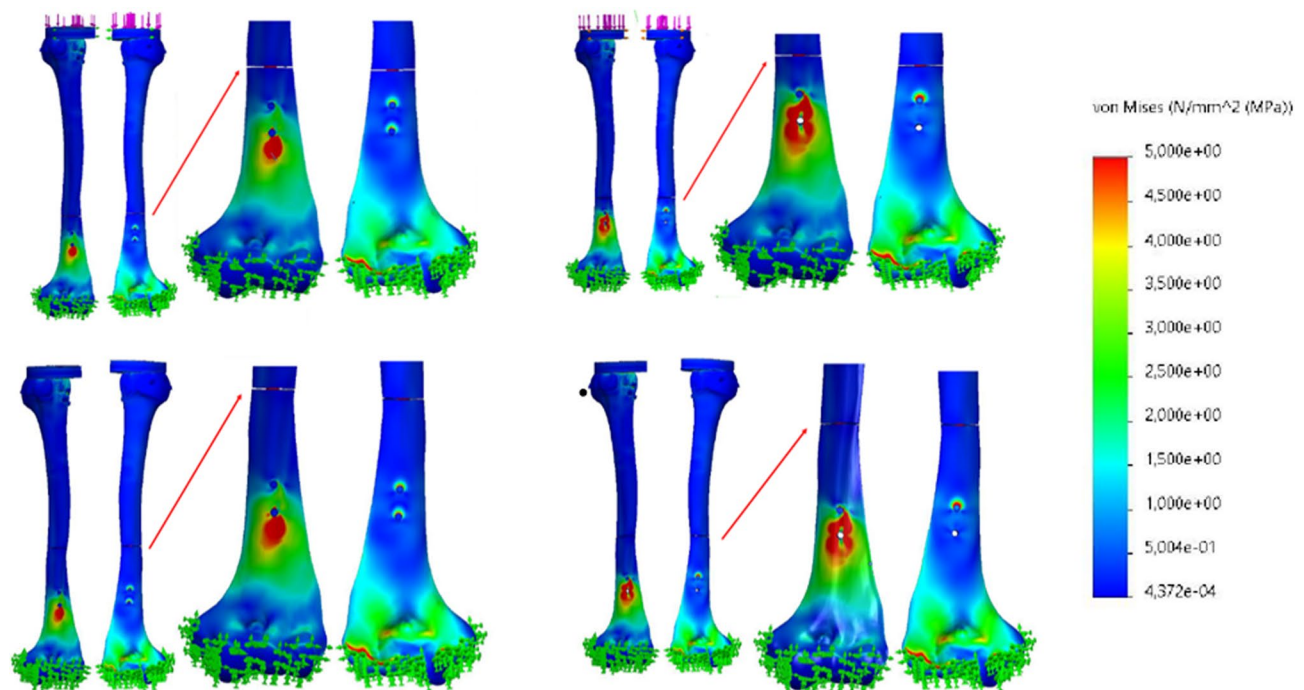


Fig. 4 At the top, from left to right: The bone tension under a compressive load with a 2 cm osteotomy changes with the number of distal screws. At the bottom, from left to right: Same for the 5 cm osteotomy configuration. On the right, the von Mises stress measured under compression

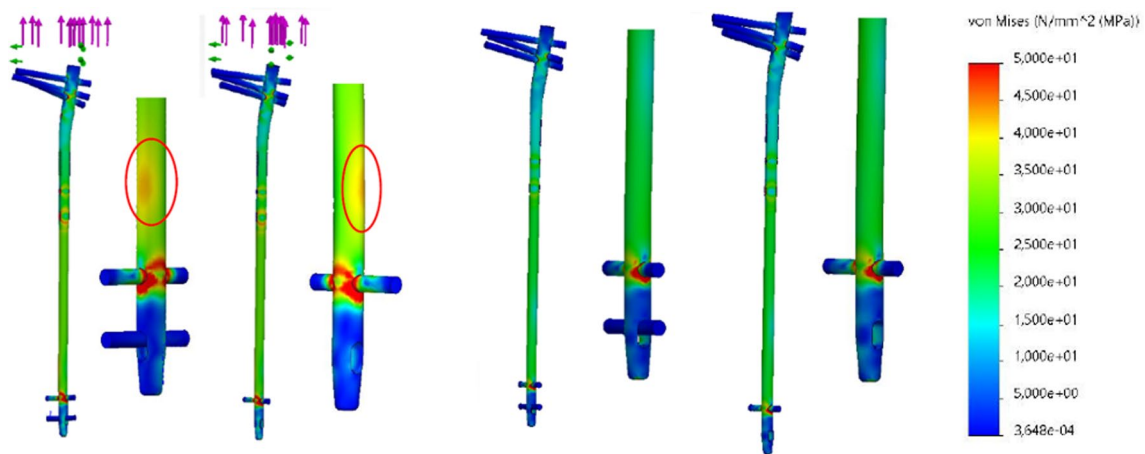


Fig. 5 An increase in the tension of the nail under traction near the osteotomy in the 2 cm osteotomy configuration (on the left), which is missing in the 5 cm osteotomy (on the right). When the tension of the proximal distal locking screw is greater (55,37 MPa for 2 cm, 49,85 MPa for 5 cm), the stiffness of the bone concentrates the loading forces on the proximal screw

Table 2 The displacement (mm) measures at osteotomy level and load level by load and osteotomy configuration

	Traction 500 N	Compression 500 N	Torsion 3Nm
Osteotomy 2 cm	0,09	0,07	0,02
Osteotomy 5 cm	0,07	0,06	0,02
Load Level 2 cm	0,1	0,08	0,05
Load Level 5 cm	0,08	0,08	0,05

Table 3 Average axial stiffness (N/mm) and displacement (mm) under traction 500 N load configuration

Load configuration	Load configuration			
	2 cm/2screw	5 cm/2screw	2 cm/1screw	5 cm/1screw
Axial Stiffness (N/mm)	932±124	1039±101	871±57	1020±90
Displacement (mm)	0.118±0.059	0.062±0.002	0.150±0.025	0.072±0.006

Table 4 Average compressive stiffness (N/mm) and displacement (mm) under compression 500 N load configuration

Load configuration	Load configuration			
	2 cm/2screw	5 cm/2screw	2 cm/1screw	5 cm/1screw
Compressive Stiffness (N/mm)	1539±139	1569±160	1473±90	1207±412
Displacement (mm)	0.073±0.026	0.087±0.025	0.098±0.002	0.116±0.006

($p=0.0034$) and 5 cm osteotomy/1 screw and 2 cm/1 screw ($p=0.0058$) cases.

Table 4 shows the average compressive stiffness and displacement data for the compressive load of 500 N. ANOVA revealed a statistically significant relationship

Table 5 Average torsional stiffness (Nm/deg) under torsion 3.00Nm load configuration

Torsional stiffness (Nm/deg)	Torsional stiffness (Nm/deg)			
	2 cm/2screw	5 cm/2screw	2 cm/1screw	5 cm/1screw
Torsion 3.00Nm	0.49±0.03	0.57±0.08	0.51±0.08	0.64±0.02

between displacement and the number of distal screws ($p=0.035$), while the associations between the displacement and osteotomy ($p=0.177$) and between osteotomy and the number of distal screws ($p=0.902$) were not significant. The application of the Bonferroni test does not show statistically significant differences.

Table 5 shows the average torsional stiffness of the 3.00 Nm torsion test.

The ANOVA results of the 3.00 Nm torsion test revealed statistically relevant relationships between the torsional stiffness and osteotomy ($p=0.015$), while the relationship between the torsional stiffness and distal screw number ($p=0.181$) and osteotomy and distal screw number ($p=0.470$) were not significant. The application of the Bonferroni test confirmed the statistically significant difference between the 2 cm osteotomy/2 screws and 5 cm osteotomy/1 screw ($p=0.0012$).

Discussion

Intramedullary nailing offers advantages such as reduced soft tissue damage and postoperative blood loss and enables early mobilization [20]. Nevertheless, complications such as radial nerve injury (7.8%) [20] and pseudoarthrosis [6] remain prevalent. Surgical technique is recognized as a modifiable factor influencing the delay in consolidation, while nonmodifiable factors include sex, smoking status, and comorbidities [21]. The healing of fractures is heavily reliant on the osteosynthesis stability [22] and the devices themselves [23, 24].

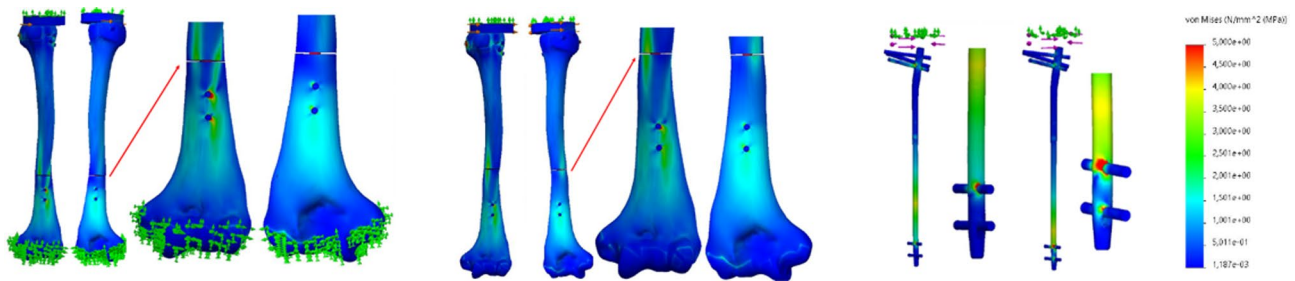


Fig. 6 The tension of the bone under torsion. On the right: The tension of the nail varying the level of osteotomy. We noted an increase near the osteotomy, which was more pronounced in the 2 cm osteotomy/2 screw configuration. When the tension near the first locking screw is greater (~ 65 Nm), and the stiffness of the bone increases the load forces on the proximal screw

The humerus, a long bone of the upper limb, experiences greater torsional forces than load forces (which are typically less than 50% of body weight) and axial forces [25, 26]. Biomechanical studies indicate that a healthy humerus possesses a torsional stiffness of $2800 \text{ N}\cdot\text{mm}/^\circ$ [27]. During preoperative planning, it is essential to consider such forces during testing and movement to achieve durable osteosynthesis, reduce stress on fracture rims, and prevent implant failure. Intramedullary nail osteosynthesis with proximal and distal locking screw systems enhances implant stability and torsional stiffness and prevents deformities such as shortening and elongation [29].

Our analysis indicated that osteosynthesis stability is influenced by the level of osteotomy and the number of distal screws. Specifically, a distance of 5 cm between the fracture plane and the proximal screw of the distal lock offers a better axial load stability than that with a distance of 2 cm. According to the FEM analysis under a 500 N traction, a lower von Mises stress was observed in the 5 cm osteotomy configuration, along with a lesser increase in the tension of the nail at the osteotomy level. The nonlinear, axially symmetric geometry of the nail and bone leads to elastic bending under axial force. A 5 cm distance between the osteotomy and distal locking screws reduces the flexural contribution, resulting in more uniform stimulation of the nail and screws throughout the implant. Consequently, the displacement is 10% lower in the 5 cm configuration. The average axial stiffness and displacement for the 5 cm configuration outperform those of the 2 cm configuration (5 cm osteotomy/2 screws $1039 \pm 101 \text{ N/mm}$, 0.062 mm ; 5 cm osteotomy/1 screw $1020 \pm 90 \text{ N/mm}$, 0.072 mm) (Fig. 5). The ANOVA results confirmed this ($p=0.006$), with the Bonferroni test indicating positive comparisons between the 5 cm osteotomy/2 screw and 2 cm/1 screw configurations and 5 cm osteotomy/1 screw and 2 cm/1 screw configurations, underscoring lower displacement with the 5 cm osteotomy.

While axial stability is primarily influenced by the distance between the fracture and the distal locking screws, compressive stability depends more on the number of

distal locking screws. FEM analysis under a compressive load of 500 N revealed slightly lower tension in the case of a 5 cm osteotomy, but the primary variation arises from the number of distal locking screws. The average displacement is $0.073 \pm 0.026 \text{ mm}$ in the 2 cm osteotomy/2 screw configuration, which is lower than the $0.116 \pm 0.006 \text{ mm}$ in the 5 cm osteotomy/1 screw configuration. Additionally, the compressive stiffness varied considerably ($1539 \pm 139 \text{ N/mm}$ for 2 cm osteotomy/2 screws and $1207 \pm 412 \text{ N/mm}$ for 5 cm osteotomy/1 screw). Displacement is lower with double distal locking screws and a 5 cm osteotomy, with an 8% reduction compared to a 10% reduction in the case of a 2 cm osteotomy. ANOVA ($p=0.03$) confirmed the significant effect of the number of distal locking screws. However, the Bonferroni test did not reveal significant correlations between different loading configurations.

FEM analysis under a torsional load of 3 Nm demonstrated greater bone tension in the 2 cm osteotomy configuration, particularly along the distal portion of the proximal fracture fragment (Fig. 6). Increasing the distance mitigates these variations, leading to greater stability of the construct. The displacement of the osteotomy stumps is almost zero, with no significant differences between the two osteotomy configurations. Analysis under torsions of 3.00 Nm revealed a complex relationship between construct stability and the influence of distal screws and the osteotomy level. The average torsional stiffness of the 5 cm osteotomy/1 screw configuration ($0.64 \pm 0.02 \text{ Nm}/^\circ$) is higher compared to the other configurations. Increasing the distance between the fracture plane and proximal screw mitigates the torsional contribution due to the model geometry, resulting in greater construct stability and lower tension. The proximal distal locking screw bears the majority of the torsional forces, thus playing a pivotal role in defining torsional stiffness, as evidenced by the FEM analysis under a torsional load. With a second distal locking screw, there is a decrease in the average torsional stiffness. The greater torsional stability with a single distal locking screw is not fully understood, and different hypotheses have been proposed

to explain this phenomenon. This could be due to the reduced elasticity of the model with a double distal locking system, leading to a decreased ability to withstand loads without undergoing permanent plastic deformation. Alternatively, it might reduce frictional forces between fracture fragments, another factor influencing torsional stiffness.

Our statistical analysis did not reveal a significant interaction effect between the number of screws and the osteotomy level on the displacement or load stiffness across the tests with different loading conditions. This lack of significance could be attributed to the small number of models analysed, a limitation of our study.

Examining changes in bone and nail tension under the three loading configurations, we noted greater tension in the distal bone fragment. Transitioning from a 2 cm osteotomy to a 5 cm osteotomy resulted in a reduced nail tension at the osteotomy level and a decreased bone tension beneath the nail. Peri-implant fractures in the humerus are rare but challenging, as evidenced by the limited literature available on this topic.

Divecha et al. [30] reported a case of a supracondylar peri-implant fracture resulting from humerus nailing. According to our FEM analysis, a 5 cm distance from the fracture to the distal screw could reduce the incidence of peri-implant fractures due to lower tension. However, no differences were observed concerning the number of distal locking screws, with the proximal screw bearing the majority of the load and no significant change in bone and nail tension upon removing the distal screw.

Limitations

This study used synthetic sawbones, which, although standardized and reproducible, do not mimic the heterogeneity and anisotropic properties of human bone. Their mechanical response under repeated load cycles may not parallel biological bone behavior. Although sawbones reduce inter-specimen variability compared to cadaveric bones, this choice limits clinical extrapolation—particularly for subtle differences that may reach statistical significance but lack clinical relevance. The reported is in accordance with the recent literature [31–33].

Moreover, mechanical testing, included repeated load cycles (3 repetitions of 5 cycles), may not affect material fatigue in the sawbone structure as mentioned in the present work [34]. Notwithstanding, no formal validation was found confirming that repeated testing does not alter performance over time in sawbone models, especially under modified configurations.

Notably, the same sawbones were re-tested after distal screw removal as in the clinical practice of nail dynamization. While this allowed comparisons between single and double locking screw configurations, the presence of pre-existing screw holes and prior loading could have

affected the results of subsequent tests. This represents a potential source of bias that should be accounted for in interpreting findings.

The study presents new biomechanical understanding of how fracture-to-screw distance and distal locking screw location affect implant stability in humeral shaft fractures. A major improvement over strictly clinical or retrospective studies, the research provides a quantifiable, repeatable method for assessing various implant designs by fusing FEM models with mechanical testing. Standardized loading conditions and verified testing procedures improve the findings' repeatability and dependability.

To confirm these results, more cadaveric and clinical research that takes patient outcomes, healing reactions, and changes in bone quality into account is required. Functional recovery, nonunion risk, and implant failure rates should all be evaluated in long-term clinical studies.

Conclusion

This study demonstrated that increasing the distance between the fracture plane and the proximal distal locking screw to 5 cm was associated with enhanced axial and torsional stability in a standardized mechanical model. Additionally, using two distal screws improved compressive stiffness compared to a single screw. These findings offer valuable biomechanical insights into the construct behavior of humeral nails under different loading scenarios. However, due to the simplified nature of the sawbone models and potential testing biases, further cadaveric and clinical studies are needed before drawing definitive conclusions about surgical practice.

Abbreviations

FEM	Finite Element Method
ORIF	Open Reduction and Internal Fixation
CRIF	Closed Reduction and Internal Fixation
AO	Arbeitsgemeinschaft für Osteosynthesefragen

Acknowledgements

We would like to thank all the participants of this study.

Author contributions

GM, MM, CG, VS, and FA were involved in the conception of this study; MM, FI, LM, and LS significantly contributed to the design of the study; GM, VP, MC and FI were involved in the data acquisition and analysis; all the authors contributed to the interpretation of the data; CG drafted the manuscript; and VP substantively revised the manuscript. All authors have approved the submitted version (and any substantially modified version that involved their contribution to the study). All authors have agreed both to be personally accountable for their own contributions and to ensure that questions related to the accuracy or integrity of any part of the work, even those in which the author was not personally involved, are appropriately investigated and resolved and that the resolution is documented in the literature.

Funding

The authors declare that no funds, grants, or other support was received during the preparation of this manuscript.

Data availability

The datasets used and/or analysed during the current study are available from the corresponding author upon reasonable request.

Declarations

Ethical approval and consent to participate

This study has been certified by the Ethics Committee of the Foggia University Hospital, Protocol No. 26/CE/2022–04 October 2022. Informed consent was obtained from all subjects involved in the study.

Consent of publication

Not applicable.

Competing interests

The authors declare no competing interests.

Received: 13 November 2023 / Accepted: 29 April 2025

Published online: 10 May 2025

References

1. Fan Y, Li YW, Zhang HB, Liu JF, Han XM, Chang X, et al. Management of humeral shaft fractures with intramedullary interlocking nail versus locking compression plate. *Orthopedics*. 2015;38(9):e825–9.
2. Gallusser N, Barimani B, Vauclair F. Humeral shaft fractures. *EFORT Open Rev*. 2021;6(1):24–34.
3. Sarmiento A, Kinman PB, Galvin EG, Schmitt RH, Phillips JG. Functional bracing of fractures of the shaft of the humerus. *J Bone Joint Surg Am*. 1977;59(5):596–601.
4. Yeh KL, Liaw CK, Wu TY, Chen CP. Radial nerve recovery following closed nailing of humeral shaft fractures without radial nerve exploration: A retrospective study. *World J Clin Cases*. 2021;9(27):8044–50.
5. Campochiaro G, Baudi P, Gialdini M, Corradini A, Duca V, Rebuzzi M, et al. Humeral shaft non-union after intramedullary nailing. *Musculoskelet Surg*. 2017;101(2):189–93.
6. Kocalkowski C, Sheridan B. Humeral shaft fractures: how effective really is functional bracing? *Shoulder Elb*. 2021;13(6):620–6.
7. Zhang R, Yin Y, Li S, Hou Z, Jin L, Zhang Y. Intramedullary nailing versus a locking compression plate for humeral shaft fracture (AO/OTA 12-A and B): A retrospective study. *Orthop Traumatol Surg Res*. 2020;106(7):1391–7.
8. Maccagnano G, Solarino G, Pesce V, Vicenti G, Coviello M, Nappi VS, et al. Plate vs reverse shoulder arthroplasty for proximal humeral fractures: the psychological health influence the choice of device? *World J Orthop*. 2022;13(3):297–306.
9. Rovere G, Meschini C, Piazza P, Messina F, Caredda M, De Marco D, et al. Proximal humerus fractures treatment in adult patients with bone metastasis. *Eur Rev Med Pharmacol Sci*. 2022;26(1 Suppl):100–5.
10. Schwab TR, Stillhard PF, Schibli S, Furrer M, Sommer C. Radial nerve palsy in humeral shaft fractures with internal fixation: analysis of management and outcome. *Eur J Trauma Emerg Surg*. 2018;44(2):235–43.
11. Foster AL, Moriarty TF, Zalavras C, Morgenstern M, Jaiprakash A, Crawford R, et al. The influence of Biomechanical stability on bone healing and fracture-related infection: the legacy of Stephan Perren. *Injury*. 2021;52(1):43–52.
12. Anteiker SB, Burden RL, Voor MJ, Roberts CS. Mechanical study of the safe distance between distal femoral fracture site and distal locking screws in antegrade intramedullary nailing. *J Orthop Trauma*. 2005;19(10):693–7.
13. Reichert P, Wnukiewicz W, Witkowski J, Bocheńska A, Mizia S, Gosk J, et al. Causes of secondary radial nerve palsy and results of treatment. *Med Sci Monit*. 2016;22:554–62.
14. Dar FH, Meakin JR, Aspdren RM. Statistical methods in finite element analysis. *J Biomech*. 2002;35(9):1155–61.
15. Noia G, Maccagnano G, Sarni L, Stigliani C, Colacicco G, Quitadamo R, et al. Biomechanical study of shaft fracture with the butterfly fragment: software simulation. *J Biol Regul Homeost Agents*. 2020;34(5 Suppl 1):107–12. IORS Special Issue on Orthopedics.
16. informations Sb. [Available from: <https://www.sawbones.com/biomechanical-product-info>
17. Data MMP. [Available from: <https://www.matweb.com>
18. Erden T, Kapicioglu M, Demirtas A, Bilsel K, Akpinar F, Kuduz H. Biomechanical comparison of humeral nails with different distal locking mechanisms: Insafeck nails versus conventional locking nails. *Acta Orthop Traumatol Turc*. 2019;53(6):490–6.
19. Garnavos C, Kanakaris NK, Lasanianos NG, Tzortzi P, West RM. New classification system for long-bone fractures supplementing the AO/OTA classification. *Orthopedics*. 2012;35(5):e709–19.
20. Ulstrup A. Secondary radial neuropathy after closed intramedullary nailing of humeral shaft fractures. Results over a 10-year period. *Acta Orthop Belg*. 2021;87(3):495–500.
21. Mills LA, Aitken SA, Simpson AHRW. The risk of non-union per fracture: current Myths and revised figures from a population of over 4 million adults. *Acta Orthop*. 2017;88(4):434–9.
22. Millar MJ, Wilkinson A, Navarre P, Steiner J, Vohora A, Hardidge A, et al. Nail fit: does nail diameter to Canal ratio predict the need for exchange nailing in the setting of aseptic, hypertrophic femoral nonunions?? *J Orthop Trauma*. 2018;32(5):245–50.
23. Kyle RF. Biomechanics of intramedullary fracture fixation. *Orthopedics*. 1985;8(11):1356–9.
24. Tarr RR, Wiss DA. The mechanics and biology of intramedullary fracture fixation. *Clin Orthop Relat Res*. 1986;212:10–7.
25. Benegas E, Ferreira Neto AA, Gracitelli ME, Malavolta EA, Assunção JH, Prada FS, et al. Shoulder function after surgical treatment of displaced fractures of the humeral shaft: a randomized trial comparing antegrade intramedullary nailing with minimally invasive plate osteosynthesis. *J Shoulder Elb Surg*. 2014;23(6):767–74.
26. Goh JC, Toh SL, Bose K. Biomechanical study on axillary crutches during single-leg swing-through gait. *Prosthet Orthot Int*. 1986;10(2):89–95.
27. Seidel H. Humeral locking nail: a preliminary report. *Orthopedics*. 1989;12(2):219–26.
28. Zimmerman MC, Waite AM, Deehan M, Tovey J, Oppenheim W. A Biomechanical analysis of four humeral fracture fixation systems. *J Orthop Trauma*. 1994;8(3):233–9.
29. Blum J, Karagül G, Sternstein W, Rommens PM. Bending and torsional stiffness in cadaver humeri fixed with a self-locking expandable or interlocking nail system: a mechanical study. *J Orthop Trauma*. 2005;19(8):535–42.
30. Divecha HM, Marynissen HA. Distal humeral fixation of an intramedullary nail periprosthetic fracture. *Case Rep Orthop*. 2013;2013:690906.
31. Cristofolini L, Schileo E, Juszczak M, Taddei F, Martelli S, Viceconti M. Mechanical testing of bones: the positive synergy of finite-element models and in vitro experiments. *Philos Trans Math Phys Eng Sci*. 2010;368(1920):2725–63.
32. Reed JR, Stanbury SJ, Menorca RM, Elfar JC. The emerging utility of composite bone models in Biomechanical studies of the hand and upper extremity. *J Hand Surg Am*. 2013;38(3):583.
33. Cristofolini L, Viceconti M, Cappello A, Toni A. Mechanical validation of whole bone composite femur models. *J Biomech*. 1996;29(4):525–35.
34. De Villiers DJ, Loh B, Tacey M, Keith P. Proximal versus distal screw placement for biceps tenodesis: a Biomechanical study. *J Orthop Surg (Hong Kong)*. 2016;24(2):258–6135.
35. Füchtmeier B, May R, Hente R, Maghsudi M, Völk M, Hammer J, Nerlich M, Prantl L. Proximal humerus fractures: a comparative Biomechanical analysis of intra and extramedullary implants. *Arch Orthop Trauma Surg*. 2007;127(6):441–7.

Publisher's note

Springer Nature remains neutral with regard to jurisdictional claims in published maps and institutional affiliations.